Interactions between transmembrane proteins embedded in a lamellar phase, stabilized by steric interactions

N. Taulier[1], M. Waks[2], T. Gulik-Krzywicki[3] and W. Urbach[4]

[1] *Department of Pharmaceutical Sciences, Faculty of Pharmacy, University of Toronto*
19 Russell Street, Toronto, Ontario, M5S 2S2 Canada
[2] *Laboratoire d'Imagerie Paramétrique, UMR 7623 CNRS*
15 rue de l'École de Médecine, 75270 Paris Cedex 06, France
[3] *Centre de Génétique Moléculaire, UPR 2420 CNRS - 91190 Gif-sur-Yvette, France*
[4] *Laboratoire de Physique Statistique de l'École Normale Supérieure, UMR 8550 CNRS*
24 rue Lhomond, 75231 Paris Cedex 05, France

Abstract. – We have investigated the distribution of the transmembrane myelin proteolipid protein when inserted into an oil-swollen lamellar phase, stabilized by steric interactions. When the hydrophobic membrane thickness, D, is larger than the hydrophobic length of the protein, d_π, only repulsive interactions are found between proteins. The repulsive forces are of electrostatic nature, arising from charges carried by the protein. The interaction potential between proteins, deduced from digitized freeze-fracture micrographs, is well fitted when the classical screened electrostatic model is used. When D is smaller than d_π, an attractive force is observed in addition to the repulsive electrostatic interactions. The attractive force originates from the membranes fluctuations. The model of membrane-mediated interactions due to the membrane thermal undulations permits us to describe our results when used in combination with the electrostatic potential.

Introduction. – Artificial inclusion assemblies within surfactant bilayers have potential applications in chemical and pharmaceutical industry [1, 2]. The correct design of such assemblies requires the understanding of the mechanism by which inclusions modify membrane properties and how a membrane contributes to the interactions between inclusions. The forces existing between them can be divided into two types: the direct and indirect interactions. The first include the short-range hydration and structural forces, van der Waals forces, and also Coulombic interactions. The second class includes long-range interactions mediated by the membranes, which are responsible for the inhomogeneous lateral distribution of proteins. Recently, it has been suggested that these significant long-range interactions are induced by two main mechanisms. In the first mechanism, the mismatch between the membrane hydrophobic thickness and the hydrophobic length of the protein leads to a membrane deformation,
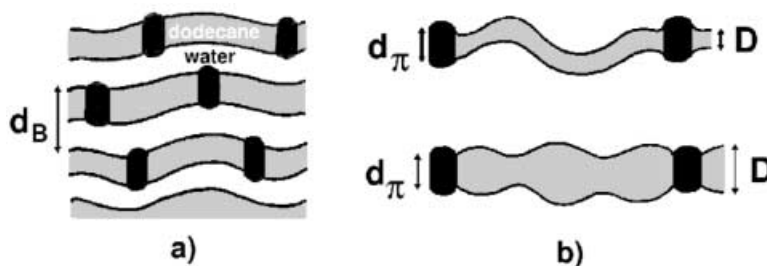
Fig. 1 – a) Schematic cartoons of the system; b) the top figure is for $D < d_\pi$, the bottom figure is for $D > d_\pi$. In the former case, the two monolayers of the membrane fluctuate cooperatively, whereas in the latter case we expect the two monolayers to fluctuate independently.

in the vicinity of the inclusion. The deformation originates from a perturbation of the constituting surfactant molecules around the inclusion, which tends to match its hydrophobic length (stretching or shortening, tilting or change in the molecular area). The membrane deformation induces lateral interactions between the inclusions, which have been theoretically described [3,4] and experimentally observed [5,6]. A second mechanism, which neglects the microscopic properties of the membrane, was first modeled by Goulian *et al.* [7] for a single membrane, and extended by Netz and Pincus [8] for a lamellar phase composed of a stack of membranes. According to these authors, thermal undulations of the membrane give rise to an interaction between the proteins, whose potential falls off as r^{-4} for a single membrane [7], whereas for a lamellar phase [8], the interaction potential exhibits Kelvin functions behavior [9], related to the rigidity and curvature coupling between the proteins. The first coupling always gives an attractive interaction, while the second one yields an undulating potential, repulsive at short scales. At longer distances, this interaction is larger than electrostatic and van der Waals interactions. In the present work, we report an experimental investigation about the interactions between transmembrane proteins embedded in highly fluctuating membranes, and we give evidence of the presence of attractive interactions due to the membrane thermal fluctuations.

We used a lamellar phase, composed of a stack of membranes, separated by water. Each membrane is formed by two monolayers of the nonionic surfactant $C_{12}E_4$ (tetraethylene glycol dodecyl ether) surrounding a layer of dodecane. Oil-swollen membranes have been used in order to avoid interactions due to the membrane-protein mismatch. Indeed, in such a case, the surfactant molecules avoid changes in conformation, since the oil fills out the gap between the two monolayers, adapting the thickness of the membrane to the inclusion length (fig. 1). The oil-swollen bilayer has also the advantage to yield a weak membrane rigidity (of the order of $2\,k_BT$ [10]), ideal for the aim of this study. The lamellar phase used here ($0.42 < \phi_s < 0.49$, $0.18 < \phi_w < 0.20$, and $\phi_d = 1 - \phi_s - \phi_w$, where ϕ_s, ϕ_w, and ϕ_d are the volume fractions of surfactant, water, and dodecane, respectively) was far enough from the border of any phase transition in the phase diagram [11]. Moreover, we have checked that no macroscopic transition occurs, and all small-angle X-ray scattering (SAXS) experiments performed on each sample exhibited the well-characteristic peak of a lamellar phase, without additional peaks from another phase. This fact was again confirmed by freeze-fracture electron microscopy. The different dimensions of the lamellar phase were determined by SAXS. The interlamellar distance, d_B, was determined from the position of the maximum of the first Bragg singularity. The membrane thickness, δ, was calculated from the classical dilution law $\delta = \phi_s d_B$. The thickness of the water layer, δ_w, was then $\delta_w = d - \delta$. Finally, the hydrophobic membrane thickness was $D = \delta - 2 \times L_h$, where L_h is the length of the polar head (≈ 8 Å for $C_{12}E_4$).
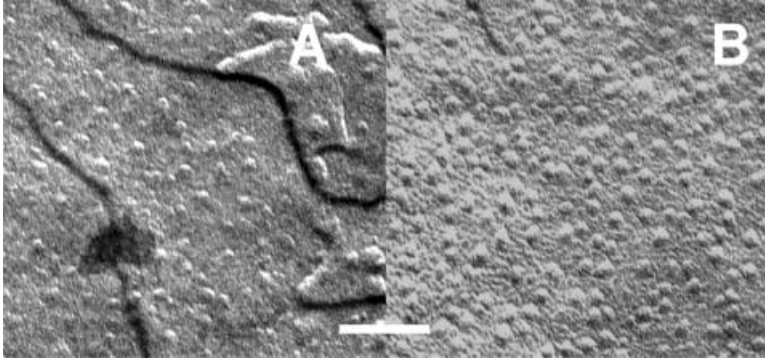
Fig. 2 – Two pictures extracted from the same micrograph for $\rho_{\text{theo}} = 0.5 \times 10^{-3}$ nm^2 and $D < d_\pi$. The scale bar represents 34 nm and the little dots are proteins. a) In this picture, the membrane is characterized by a lack of flatness and $\rho_{\text{exp}} \ll \rho_{\text{theo}}$; b) the picture exhibits a flatness membrane with $\rho_{\text{exp}} \gg \rho_{\text{theo}}$.

The transmembrane protein is the myelin proteolipid, extracted from bovine brain as described by Nicot *et al.* [12]. The proteolipid is a major transmembrane basic protein of myelin, involved in demyelinating diseases [13]. It consists of four hydrophobic α-helices, connected by charged hydrophilic peptide segments. We have previously reported [14] that the protein is not denatured upon insertion into the nonionic lamellar phase: the helices are located inside the swollen hydrophobic part of the membrane, while the hydrophilic segments are solvated in water. Under the above experimental conditions, about 10 charged lipid molecules remain tightly bound to one protein [15].

The interaction potential between transmembrane proteins can be extracted from the distribution of proteins within the membrane [6,16]. To this end, we have digitized freeze-fracture electron microscopy micrographs of the membrane (fig. 2). Freeze-fracture experiments were performed as described previously [12]. We have investigated the distribution of the protein at two different membrane dimensions ($D/d_\pi > 1$ or $D/d_\pi < 1$), and at several protein densities (table I). At least four scanned images have been treated for each sample. Between 600 and 1500 proteins were found per image, depending on its size and its magnification.

From N_S, the number of proteins on the membrane surface, S, determined from micrographs, we calculate the experimental overall surface density of proteins: $\rho_{\text{exp}} = N_S/S$. N_S

TABLE I – *Theoretical and experimental protein surface densities accompanied by the values of the hydrophobic membrane thickness, D, and the thickness of the polar layer, $D_{\text{polar}} = d_B - D$. The error on densities is about 10%. The hydrophobic length of the protein, d_π, equals 42 Å [17]. The last row is when water has been replaced by a brine solution of 20 mM NaCl.*

D (Å)	D_{polar} (Å)	ρ_{exp} (10^{-3} nm^{-2})	ρ_{theo} (10^{-3} nm^{-2})	$\rho_{\text{exp}}/\rho_{\text{theo}}$
49 ($> d_\pi$)	34	3.2	4	0.8
46 ($> d_\pi$)	31	1.5	1	1.5
38 ($< d_\pi$)	28	2.8	0.9	3.1
38 ($< d_\pi$)	28	1.6	0.5	3.2
38 ($< d_\pi$)	28 (20 mM NaCl)	2.1	0.5	4.2

can be compared to the "theoretical" density, obtained from the relationship: $\rho_{\text{theo}} = \frac{N_V}{V/d_B}$, where N_V is the number of proteins inserted in the lamellar phase. V is the volume and d_B is the Bragg distance of the lamellar phase (fig. 1). This "theoretical" density represents the case of a homogeneous distribution of proteins on the overall membrane surface. Inspection of the ratio $\rho_{\text{exp}}/\rho_{\text{theo}}$ listed in table I shows that $\rho_{\text{exp}} \approx \rho_{\text{theo}}$ when $D > d_\pi$, whereas $\rho_{\text{exp}} \gg \rho_{\text{theo}}$ when $D < d_\pi$. Specifically, for a similar "theoretical" density, $\sim 10^{-3}$ nm^{-2}, an experimental density of the same order is found (1.5×10^{-3} nm^{-2}) when $D > d_\pi$, whereas an experimental density three times larger (2.8×10^{-3} nm^{-2}) is found when $D < d_\pi$. Conversely, an experimental density of $\sim 1.5 \times 10^{-3}$ nm^{-2} is achieved with twice less proteins ($\rho_{\text{theo}} = 0.5 \times 10^{-3}$ nm^{-2}) when $D < d_\pi$ than for $D > d_\pi$ ($\rho_{\text{theo}} = 10^{-3}$ nm^{-2}).

From these observations, we conclude that only repulsive interactions take place between proteins when $D > d_\pi$. Indeed, repulsive interactions homogeneously spread the proteins on the membrane. Conversely, we conclude that a sum of attractive and repulsive interactions takes place when $D < d_\pi$, leading to a phase transition. Indeed, the attractive interaction gathers the proteins in high-density regions ($\rho_{\text{exp}} \gg \rho_{\text{theo}}$), and leaves others regions with a low density of proteins, $\rho_{\text{exp}} \ll \rho_{\text{theo}}$. Additionally, no aggregation is observed in the high-density regions because of the presence of repulsive interactions. Figure 2 shows such regions of low and high densities obtained from freeze-fracture micrographs when $D < d_\pi$. However, to achieve our treatment, we have selected only flat parts of the micrographs, which correspond to the highest protein density regions.

The interaction potential, $u(r)$, between proteins was derived from the radial correlation function $g(r)$[1], which measures the probability of finding a second protein at a distance r from a given one. The method consists in solving the system composed of the Ornstein-Zernike [18] equation $g(r) - 1 = c(r) + \rho_{\text{exp}} \int c(r')[g(r - r') - 1]\mathrm{d}r'$, and the Percus-Yevick equation [19] $c(r) = g(r)(1 - e^{\frac{u(r)}{k_B T}})$. Note that we have got the same results as presented hereafter when the hypernetted chain equation [20] is used instead of the Percus-Yevick equation. The numerical solutions were obtained using the algorithm of Lado [20].

Figures 3a) and b) show two distribution functions, $g(r)$, and two interaction potentials, $u(r)$, respectively, for both cases $D > d_\pi$ and $D < d_\pi$ when the same concentration of proteins is used (*i.e.* for the same theoretical density $\rho \approx 10^{-3}$ nm^{-2}).

Recall that for $D > d_\pi$ we have concluded that only repulsive interactions occur between the proteins from the fact that $\rho_{\text{exp}} \approx \rho_{\text{theo}}$. Since charges are carried by the myelin proteolipid, a protein-lipid complex, we expect screened repulsive electrostatic interactions between them. To confirm the presence of repulsive electrostatic interactions, we have replaced water by brine in one sample where both attractive and repulsive interactions are present (for $D < d_\pi$ and $\rho_{\text{exp}} = 0.5 \times 10^{-4}$). When 20 mM NaCl was added to water of the lamellar phase, an increase of the surface density of proteins, ρ_{exp}, was observed (from 1.6 to 2.1×10^{-3} nm^{-2}, see table I). For a higher salt concentration (> 100 mM), myelin proteolipid precipitation was observed, indicating that attractive interactions have superseded electrostatic repulsive forces, leading to aggregates. Therefore, the experimental potential $u(r)$ should contain the electrostatic potential $e\psi(r)$, the solution of the Poisson-Boltzmann (PB) equation. In the Debye-Hückel (DH) approximation, $|e\psi| \leq k_B T$, the PB equation is simply $\Delta\psi = \lambda_D^{-2}\psi$, where λ_D represents the Debye length [21]. Although the DH approximation is not strictly valid for small values of r, when the experimental interaction potential becomes of the order of a few $k_B T$, it can provide nevertheless a good approximation. Moreover, the solution $e\psi(r)$

---

[1] Experimentally $g(r)$ cannot be measured exactly, but the function $g(r, r + \delta r)$ which is the ratio of the surface density of proteins located on an annulus $S_{\text{ann}}(r, r + \delta r)$ between r and $r + \delta r$, to the overall mean density particle, ρ_{exp} can.
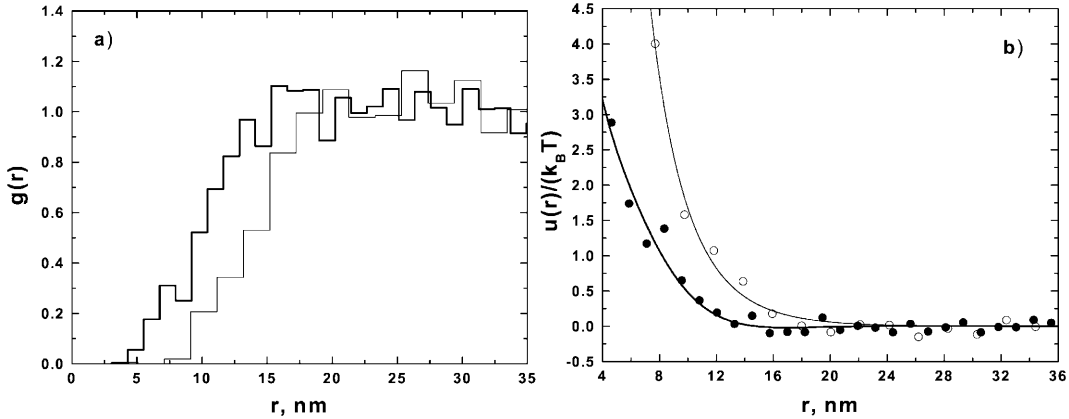
Fig. 3 – a) Distribution functions $g(r)$ for $D > d_\pi$ (thin line) and for $D < d_\pi$ (thick line). b) Interaction potentials $u(r)$ for $D > d_\pi$ (●) and for $D < d_\pi$ (○). The thin line is the best fit using the electrostatic potential $e\psi$ while the thick line is the best fit using the potential $(e\psi + u_{\text{mf}})$ (see text). All curves are derived from the same concentration of proteins (*i.e.* $\rho_{\text{theo}} \approx 10^{-3}$ nm^{-2}), but for $D > d_\pi$, $\rho_{\text{exp}} \approx \rho_{\text{theo}}$, whereas for $D < d_\pi$, $\rho_{\text{exp}} \approx 3 \times \rho_{\text{theo}}$.

depends on the dimensionality. For a two-dimensional system (when the water layer thickness is zero in our case) it has been shown that $\psi(r)$ decays algebraically [22]. Since an exponential decay $\psi(r)$ is experimentally observed for the purely repulsive case, *i.e.* $D > d_\pi$, this is a proof that a two-dimensional model is not appropriate to describe our system. Our system must rather be considered as a confined three-dimensional system. Consequently, we have used the classical three-dimensional solution to fit our data: $\psi(r) = \frac{\psi_0}{e} \frac{2r_{\text{p}}}{r} e^{-\frac{(r - 2r_{\text{p}})}{\lambda_{\text{D}}}}$, where r_{p} is the radius of the protein. We used r_{p}, ψ_0, and λ_{D} as free parameters in our fits. For $D > d_\pi$, the electrostatic solution perfectly fits the experimental interaction potential (fig. 3a).

Recall now that for $D < d_\pi$, we have previously drawn conclusions on to the presence of attractive forces in addition to repulsive interactions from the fact that the freeze-fracture micrographs exhibit regions wiht high and low densities of proteins. Additionally, we observe that, for $D < d_\pi$, all interaction potentials cannot be correctly fitted by an exponential or algebraic curve (fig. 3b)). Recall that the lamellar phase is stabilized by steric interactions [23], meaning that the membrane fluctuations are the dominant forces. It has been demonstrated by Goulian *et al.* for a single membrane and then by Netz and Pincus for a lamellar phase that membrane fluctuations induce indirect attractive interactions between the proteins. Thus, for $D < d_\pi$, we have fitted all our experimental potential with the sum of the electrostatic potential, $e\psi$, and the potential, u_{mf}, derived by Netz and Pincus. We observed that all our interactions potentials were well fitted by $(e\psi + u_{\text{mf}})$ when $D < d_\pi$ (see fig. 3b)). The potential, u_{mf}, depends on the perturbation in rigidity, $\kappa_0 + \delta\kappa$, and curvature, $c_0 + \delta c$, due to the protein, where $\kappa_0 \approx 2k_{\text{B}}T$ is the rigidity of the membrane, and c_0, the spontaneous curvature of the membrane, which is unknown:

$$u_{\text{mf}}(r) = -\frac{a^4 \delta\kappa^2 k_{\text{B}}T}{2} \left[\frac{1}{\pi\kappa_0 \xi_{||}^2} kei\left(\frac{\sqrt{2}(r - 2r_{\text{p}})}{\xi_{||}} \right) \right]^2 - \frac{a^4 \delta c^2}{\pi \xi_{||}^2} kei\left(\frac{\sqrt{2}(r - 2r_{\text{p}})}{\xi_{||}} \right), \quad (1)$$

where $\xi_{||}$ is a correlation length as defined in ref. [8]; $a^2 = \pi r_{\text{p}}^2$ is the surface area of the protein; $kei(r)$ is a Kelvin function [9]. Considering $\delta\kappa$, δc, r_{p}, and $\xi_{||}$ as free parameters, we found approximatively that $\delta\kappa \approx 25 \pm 8k_{\text{B}}T$, $\delta c \approx 1 \pm 0.5$ nm^{-1} and $\xi_{||} \approx 5 \pm 2$ nm, which
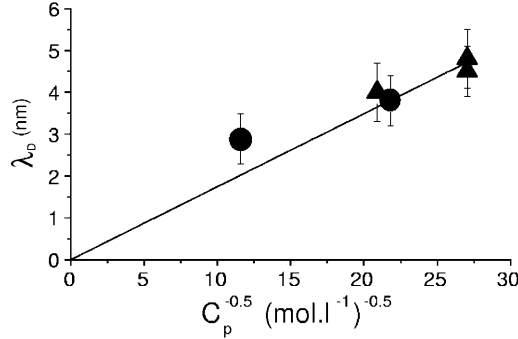
Fig. 4 – The linear variation of the Debye length, λ_D, *vs.* $1/\sqrt{C_p}$ indicates that the ions are brought by the proteins. ▲ is for $D > d_\pi$; ● is for $D < d_\pi$ and by taking into account the membrane-mediated interactions.

are reasonable values for the myelin proteolipid under study. Note that r_p is the same value in $e\psi$ and u_{mf} and the fits gave approximatively the value $2 \times r_p \approx 4.4 \pm 0.4$ nm.

One also should note that the addition of attractive and repulsive interactions does not lead to a well-defined minimum, corresponding to the mean distance between two proteins (fig. 3b)). The experimental potential is simply altered compared to the electrostatic repulsive potential. This observed characteristic is well predicted by the model of Netz and Pincus. In contrast, for $D > d_\pi$, we do not observe the presence of attractive interactions. Since membrane fluctuations are still the dominant force stabilizing the lamellar phase, we suggest that increasing the membrane thickness of the oil-swollen bilayer decouples the fluctuation of each monolayer of the membrane (see fig. 1b)). Since the fluctuations of the two monolayers are no longer cooperative, the fluctuations of the membrane become weaker, leading to the disappearance of the attractive forces, which are completely overcome by the repulsive ones.

Finally, fig. 4 displays the values of the Debye length, λ_D, obtained by fitting the experimental potential by $e\psi$ when $D > d_\pi$ and $e\psi + u_{mf}$ when $D < d_\pi$. The small values of the Debye length are in favor of a significant number of screening ions. These values are also smaller than the distance between two neighbor polar layers. This means that the screening is achieved within a polar layer, and that the neighbor polar layers do not participate in the screening. Since surfactant molecules are nonionic and the presence of ions in water is low, we expect these ions to be brought by the protein. Indeed, we observed in fig. 4 that the variation of λ_D is linear to $1/\sqrt{C_p}$, where C_p is the molar volume concentration of protein in water (with the imposed condition $\lambda_D = 0$ when $C_p \longrightarrow \infty$). The Debye length λ_D is also related to ion concentration $C = (\alpha/\lambda_D)^2$, with $\alpha = 0.304$ for a 1:1 electrolyte in water [21]. We found that the number of ions brought per protein, $Q = C/C_p$, is 3.

In conclusion, we have shown that repulsive electrostatic forces are always present in our samples, and are due to charges carried by the proteins. Specifically, we have shown that the addition of salt decreases the strength of the repulsive interactions, and in the purely repulsive case, that the experimental potential is perfectly fitted by the classical screened electrostatic potential. Additionally, the values found for the Debye length are consistent with that we know of the protein. Moreover, the presence of electrostatic interactions may explain the absence of aggregation, observed with the same proteins acting as molecular clips between surfactant lamellae, described by Taulier *et al.* [10]. This is despite the prediction of existing models [24, 25], which do not take into account such interactions.

We have further shown the existence of an attractive interaction when $D < d_\pi$, from the

presence of high and low protein surface densities from our micrographs. The fact that the lamellar phase is stabilized by membrane fluctuations suggests to us that they are responsible for the observed attractive interactions, as predicted by Netz and Pincus. Indeed, the potential of Netz and Pincus combined with the electrostatic potential successfully fit our experimental potentials.

Finally, these results could suggest that interactions, due to thermal membrane undulations, also act in myelin, a biological multilayer system. We can thus expect that similar forces are involved in the stability and the biological role of the proteolipid in central nervous system myelin.

$$* * *$$

REFERENCES

[1]   OZIN G., *Adv. Mater.*, **4** (1992) 612.
[2]   TANEV P. and PINNAVAIA T., *Science*, **271** (1996) 1267.
[3]   ABNEY J. R. and OWICKI J. C., *Progress in Protein-Lipid Interactions*, Vol. **76** (Watts/De Pont) 1985, p. 1.
[4]   ARANDA-ESPINOZA H., BERMAN A., DAN N., PINCUS P. and SAFRAN S., *Biophys. J.*, **71** (1996) 648.
[5]   HARROUN T. A., HELLER W. T., WEISS T. M., YANG L. and HUANG H. W., *Biophys. J.*, **76** (1999) 937.
[6]   PEARSON L., CHAN S., LEWIS B. and ENGELMAN D., *Biophys. J.*, **43** (1983) 167.
[7]   GOULIAN M., BRUISMA R. and PINCUS P., *Europhys. Lett.*, **22** (1993) 145.
[8]   NETZ R. and PINCUS P., *Phys. Rev. E*, **52** (1995) 4114.
[9]   ABRAMOWITZ M. and STEGUN I. A., *Handbook of Mathematical Functions* (Dover Publications, New York) 1993.
[10] TAULIER N., NICOT C., WAKS M., HODGES R. S., OBER R. and URBACH W., *Biophys. J.*, **78** (2000) 857.
[11] KUNIEDA H. *et al.*, *Langmuir*, **7** (1991) 1915.
[12] NICOT C., WAKS M., OBER R., GULIK-KRZYWICKI T. and URBACH W., *Phys. Rev. Lett.*, **77** (1996) 3485.
[13] GREER J. M., SOBEL R. A., SETTE A., SOUTHWOOD S., LEES M. B. and KUCHROO V. K., *J. Immunol.*, **156** (1996) 371.
[14] MERDAS A., GINDRE M., LE HUÉROU J.-Y., OBER R., NICOT C., URBACH W. and WAKS M., *J. Phys. Chem. B*, **102** (1998) 528.
[15] VACHER M., WAKS M. and NICOT C., *J. Neurochem.*, **52** (1989) 117.
[16] BRAUN J., ABNEY J. and OWICKI C., *Nature*, **310** (1984) 316.
[17] WEIMBS T. and STOFFEL W., *Biochemistry*, **31** (1992) 12289.
[18] ORNSTEIN L. S. and ZERNICKE F., *Proc. Acad. Sci. Amsterdam*, **17** (1914) 793.
[19] PERCUS J. and YEVICK G., *Phys. Rev.*, **110** (1958) 1.
[20] LADO F., *J. Chem. Phys.*, **49** (1968) 3092.
[21] ISRAELACHVILI J., *Intermolecular and Surface Forces*, third edition (Academic Press) 1985.
[22] MULLER V. M. and DERJAGUIN B. V., *J. Colloid Interface Sci.*, **61** (1977) 361.
[23] HELFRICH W., *Z. Naturforsch. A*, **33** (1978) 371.
[24] SENS P., TURNER M. and PINCUS P., *Phys. Rev. E*, **55** (1997) 4394.
[25] BRUISMA R., GOULIAN M. and PINCUS P., *Biophys. J.*, **67** (1994) 746.